J. Astrophys. Astr. (1988) **9,** 185–192

Vortex Rings in the Working Surface of Radio Jets

Sandip K. Chakrabarti* *International Center for Theoretical Physics, Strada Costiera 11, 34000 Trieste, Italy and Theoretical Astrophysics, California Institute of Technology, Pasadena, USA*

Received 1988 February 10; accepted 1988 July 13

Abstract. We study the effects of the presence of vortex rings surrounding a supersonic radio jet inside the cocoon of a radio lobe. We show that both the jet and the shocked ambient medium are pinched. Flow speed inside the cocoon is always close to the sonic value and it stays so by successively passing through several oblique shocks. We also discuss the possibility of the non-linear growth of the instabilities of the contact surface to explain the numerical results in the literature.

Key words: radio sources, jets—shocks—vortex rings—pinch instability

1. Introduction

It is increasingly evident from the recent numerical simulations (Norman, Winkler & Smith, 1982; Williams & Gull 1984, 1985; Norman & Winkler 1985; Lind 1986) that the working surface of a radio jet is probably far more complex than the original model of Blandford & Rees (1974). In particular, periodic shedding of vortices into the cocoon which propagate upstream of the jet is common. There is yet no conclusive evidence for these features in radio jets. Recent VLA polarization data of Cyg A by Dreher, Carilli & Perley (1987) shows the rotation measure of opposite signs to be symmetrically distributed about the axis of both the east and the west lobes indicating the presence of vortical motions. To explain laboratory experiments of production of vortex rings by Baird (1987), Broadbent & Moore (1987) calculates the effect of a single vortex ring on a supersonic jet without a cocoon. No such analysis has been carried out in the context of a radio jet where the jet is surrounded by a cocoon which is in turn surrounded by the shocked ambient medium (or, *screen* for short, see Fig. 1). In this paper we present such an analysis and show that it reproduces many features which are observed in the extensive numerical simulations. A more detailed discussion is found in Chakrabarti (1988).

2. A Pair of Vortex rings in the Cocoon

We assume that the problem is strictly two-dimensional. The unperturbed boundaries between the jet and the cocoon and the cocoon and the shocked ambient medium are

* Present address: Theoretical Astrophysics, Tata Institute of Fundamental Research, Homi Bhabha Road, Colaba, Bombay 400 005.

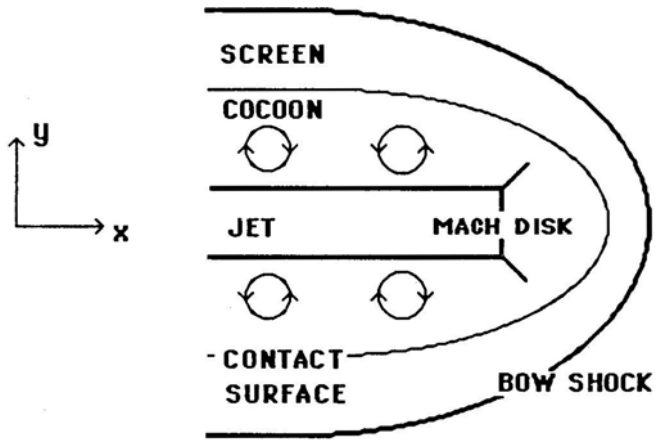

Figure 1. The schematic diagram showing the relative locatio n s of the principal components of the working surface of a radio jet.

parallel to the x-axis. The vortex rings are replaced by the line vortices which are normal to the plane of the diagram (Fig. 1). Also we assume that the strength of the vortices are small (each equal to k in analysis below) so that the perturbations can be carried out by linear analysis. The analysis is done only up to k^2 therefore ignoring the higher-order effects involving the motion of the vortex-pairs in a direction normal to the jet flow (*i.e.*, along the y-axis). All the distance scales are measured in units of the thickness of the unperturbed cocoon which is chosen to be 2π. Our coordinate system co-moves with the velocity U_r (exact number is unimportant for the present analysis) of the vortex pair with respect to infinity. Thus a pair of vortices placed at $x = \pm b$ on the $y = 0$ axis will always maintain these coordinates.

Let the subscripts s, c and j denote quantities in the screen, in the cocoon and in the jet, respectively. Also, let v_s , v_c, v_j denote the unperturbed velocities of the fluid medium in the screen, in the cocoon, and in the jet as measured in the frame of the vortices. We now expand the velocity potentials inside these three media in the following way:

$$\phi_s = v_s(x + \varepsilon_s^2 \phi_{1s} + \varepsilon_s^4 \phi_{2s} + \ldots), \tag{1}$$

$$\phi_c = v_c(x + \varepsilon_c \phi_{1c} + \varepsilon_c^3 \phi_{2c} + \ldots), \tag{2}$$

$$\phi_j = v_j(x + \varepsilon_j^2 \phi_{1j} + \varepsilon_j^4 \phi_{2j} + \ldots). \tag{3}$$

The small parameters $\varepsilon_{s,c,j}$ are defined as,

$$\varepsilon_i = \frac{\kappa}{4\pi v_i}, \tag{4}$$

where, the index i takes the values s, c and j. The quantities ϕ_1 and ϕ_2 are the correction terms due to the perturbation. Since inside the cocoon the velocity correction term must 'feel' the rotational vortex flow field, only the odd powers of ε appear in ϕ_c but since the perturbations of the flow field inside the jet and the screen are produced only via pressure (which is proportional to the square of the velocity field) variation through the boundary, only the even powers appear in ϕ_j and ϕ_s. Consequently, the equations

of the cocoon boundary and the jet boundary take the forms:

$$y_s(x)=\pi+\varepsilon_s^2\eta_{1s}(x)+\varepsilon_s^4\eta_{2s}(x)+\ \ldots\ , \tag{5}$$

and,

$$y_j(x)=-\pi+\varepsilon_j^2\eta_{1j}(x)+\varepsilon_j^4\eta_{2j}(x)+\ \ldots\ . \tag{6}$$

We use the method of images to calculate the velocity potential inside the cocoon (Lamb 1932). Thus, $\phi_{1c}=\mathrm{Re}(\omega)$, where, ω is obtained from

$$\omega\propto\log(Z\pm b)+\log(Z\pm b\pm 2\pi i)+\log(Z\pm b\pm 4\pi i)+\ \ldots\ , \tag{7}$$

Z being the complex coordinate $x + iy$. The velocity components turn out to be

$$v_x=\frac{\kappa}{4\pi}\left[\frac{\mathrm{sh}(x-b)}{\mathrm{ch}(x-b)-\cos y}\pm\frac{\mathrm{sh}(x+b)}{\mathrm{ch}(x+b)-\cos y}\right]+v_c, \tag{8}$$

and

$$v_y=\frac{\kappa}{4\pi}\left[\frac{\sin y}{\mathrm{ch}(x-b)-\cos y}\pm\frac{\sin y}{\mathrm{ch}(x+b)-\cos y}\right], \tag{9}$$

where the upper sign is to be used when both the vortices have strength $k > 0$ and the lower sign is to be used when the strengths are opposite (in the sense shown in Fig. 2a,b).

From the Bernoulli's equation the pressure variation inside the cocoon is written as,

$$\frac{P_c}{\rho_c}+\frac{1}{2}(v_x^2+v_y^2)=\frac{P_{\infty c}}{\rho_c}+\frac{1}{2}\left(\frac{\kappa^2}{16\pi^2}+v_c^2\right). \tag{10}$$

The x-component of velocity at infinity is $k/4\pi$.We have considered here the flow to be locally incompressible so that density ρ can be treated as constant. $P_{\infty c}$ is the pressure in the cocoon at infinity. We now define the pressure coefficients,

$$C_{ps}=\frac{(P_c-P_{\infty c})}{\frac{1}{2}\rho_s v_s^2}, \tag{11}$$

and

$$C_{pj}=\frac{(P_c-P_{\infty c})}{\frac{1}{2}\rho_j v_j^2}. \tag{12}$$

To the leading order, the pressure coefficients could be equated to $C_{ps} = -2\varepsilon_s^2\partial\phi_{1s}/\partial x$ and, $C_{pj} = -2\varepsilon_j^2\partial\phi_{1j}/\partial x$ (Liepman & Roshko 1956) at the screen boundary at $y= \pi$ and the jet boundary at $y = -\pi$ respectively. Substituting these partial derivatives in the wave equations for the perturbation

$$m_s^2\frac{\partial^2\phi_{1s}}{\partial x^2}=\frac{\partial^2\phi_{1s}}{\partial y^2}, \tag{13}$$

and

$$m_j^2\frac{\partial^2\phi_{1j}}{\partial x^2}=\frac{\partial^2\phi_{1j}}{\partial y^2}, \tag{14}$$

where $m_s^2 = M_{\infty s}^2 - 1$ and $m_j^2 = M_{\infty j}^2 - 1$ here M_∞ denotes the Mach number of the flow at a large distance. The equations of the screen and the jet boundary are obtained

by using the pressure balance conditions at each boundary, i.e.,

$$\frac{\partial \phi_s}{\partial y}\Big/\frac{\partial \phi_s}{\partial x} = \varepsilon_s^2 \frac{\partial \eta_{1s}}{\partial x} + \varepsilon_s^4 \frac{\partial \eta_{2s}}{\partial x} + \ldots, \tag{15}$$

$$\frac{\partial \phi_j}{\partial y}\Big/\frac{\partial \phi_j}{\partial x} = \varepsilon_j^2 \frac{\partial \eta_{1j}}{\partial x} + \varepsilon_j^4 \frac{\partial \eta_{2j}}{\partial x} + \ldots. \tag{16}$$

Substituting the expressions for ϕ_s and ϕ_j in the above equations and equating terms of order ε_s^2 and ε_j^2 one obtains,

$$\frac{\partial \eta_{1s}}{\partial x} = \frac{\partial \phi_{1s}}{\partial y}\bigg|_{y=\pi} = \pm m_s \frac{\partial \phi_{1s}}{\partial x}\bigg|_{y=\pi}, \tag{17}$$

and

$$\frac{\partial \eta_{1j}}{\partial x} = \frac{\partial \phi_{1j}}{\partial y}\bigg|_{y=-\pi} = \pm m_j \frac{\partial \phi_{1j}}{\partial x}\bigg|_{y=-\pi}. \tag{18}$$

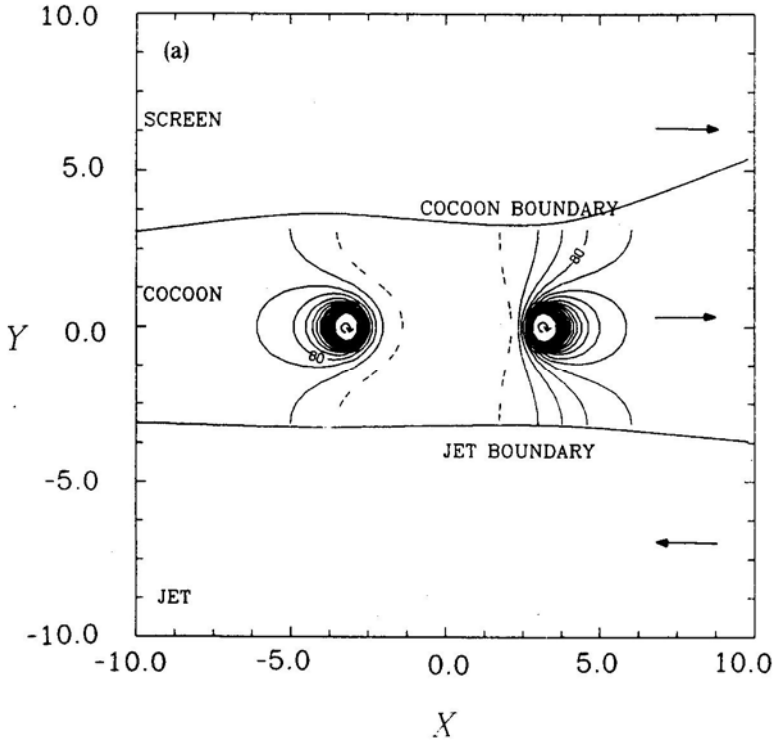

Figure 2. The nature of the perturbation of the jet boundary and the cocoon boundary are shown when a pair of vortex rings with a) same vorticity, and b) opposite vorticity are introduced in the cocoon. The fluid flows towards right both in the cocoon and in the screen and towards left in the jet. The parameters are: $4\pi\nu_c/k$ =0.4, q_s=0.16, q_j=0.04, $P_{\infty c}$ = 0.2.The contours of the constant Mach numbers are equally spaced in logarithmic scale with interval 0.003. Dashed lines correspond to subsonic motion. The contours marked 80 are for $\log_{10}(M_c) = 0.008$.

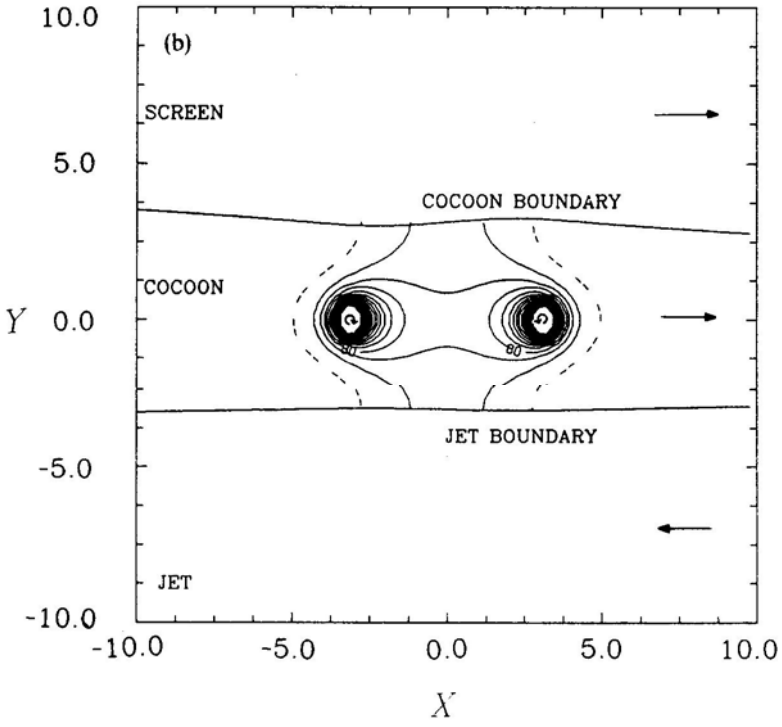

Figure 2. Continued.

Upon integration one obtains the equations for the boundary corrected up to k^2 of the screen as,

$$y_s(x)=\pi\mp q_s\left[-\left(3+\frac{16\pi^2v_c^2}{\kappa^2}\right)\frac{x}{2}+\mathrm{th}\frac{x-b}{2}+\mathrm{th}\frac{x+b}{2}\right.$$
$$\left.+2\left(\frac{1}{\mathrm{th}b}-\frac{4\pi v_c}{\kappa}\right)\log\mathrm{ch}\frac{x+b}{2}-2\left(\frac{1}{\mathrm{th}\,b}+\frac{4\pi v_c}{\kappa}\right)\log\mathrm{ch}\frac{x-b}{2}\right] \tag{19}$$

when both the vortices are of same sign and,

$$y_s(x)=\pi\mp q_s\left[\left(1-\frac{16\pi^2v_c^2}{\kappa^2}\right)\frac{x}{2}+\mathrm{th}\frac{x-b}{2}+\mathrm{th}\frac{x+b}{2}\right.$$
$$\left.-2\left(\frac{1}{\mathrm{th}\,b}-\frac{4\pi v_c}{\kappa}\right)\log\frac{\mathrm{ch}\frac{x+b}{2}}{\mathrm{ch}\frac{x-b}{2}}\right] \tag{20}$$

when the vorticities are of opposite signs Here $q_s = \varepsilon_s^2 m_s\rho_c/\rho_s$. By replacing q_s by q_j one obtains similar results for the jet boundary. The variation of the Mach number with pressure is obtained from Equation (10) as,

$$P_c[1+\tfrac{1}{2}(\gamma-1)M_c^2]^{\frac{\gamma}{\gamma-1}}=P_{\infty c}[1+\tfrac{1}{2}(\gamma-1)M_{\infty c}^2]^{\frac{\gamma}{\gamma-1}}. \tag{21}$$

The subscript ∞ refer to quantities at a large distance from the vortices. The contours of constant Mach numbers are shown in Figs 2a,b. Fig. 2a is for vortices of the same

sign and Fig. 2b is for vortices with opposite signs. The value of b was chosen to be π. Solid lines are for $M_c > 1$ and dashed lines are for $M_c < 1$. The contours are of equal logarithmic interval and the ones marked 80 are for $\log_{10}M_c = 0.008$. The ratio $q_s/q_j = 4$ is considered in this particular case.

In both the Figs 2a and b we notice that the nature of the velocity field is very much different from that of a uniform flow. Because of the large momentum flux in the jet, the pinching of the jet boundary is much smaller than that of the cocoon boundary. The magnitude of the pinching is determined by the quantities q_s and q_j which are functions of the density, velocity, Mach number of the flow and the strength of the vortices. The velocities inside the cocoon and the screen are positive towards the positive x-axis and that of the jet is along the negative x-axis. In Fig. 2a the jet expands downstream by depositing momentum in the cocoon whereas in Fig. 2b the jet is collinated (albeit very

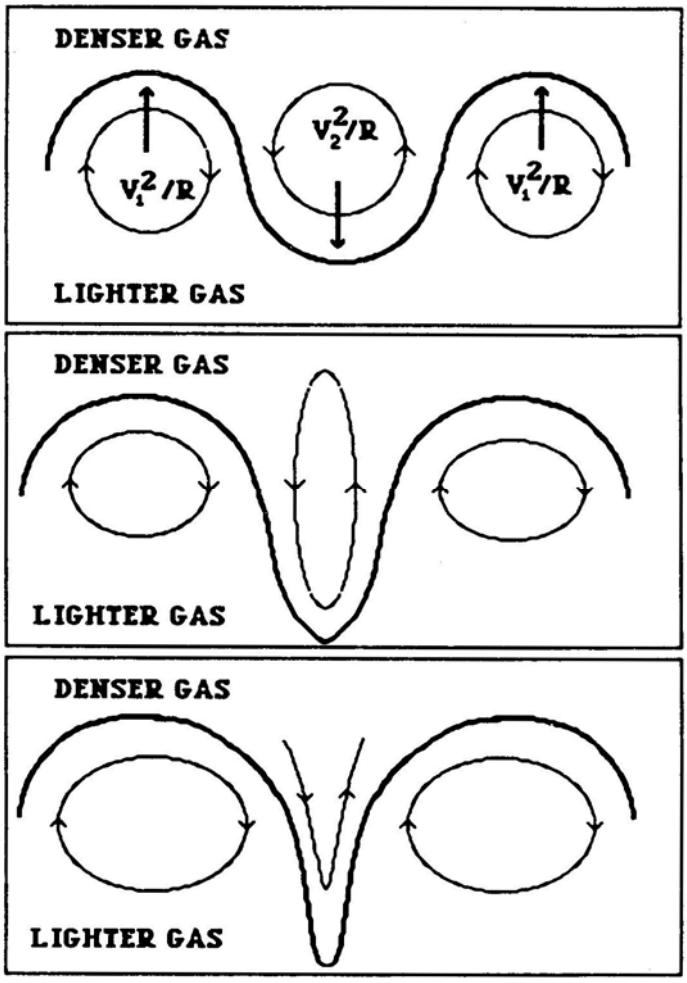

Figure 3. Plausible mechanism for production of 'spikes' on the contact discontinuity. The Rayleigh-Taylor instability is selectively turned on whenever the local gravity due to the centrifugal acceleration points from heavy fluid to the light fluid.

slowly). The perturbation propagates downstream indefinitely in this model but in reality it passes through the terminating shock called the Mach disc. The expansion and collimation of the jet show that the kinetic luminosity is affected by the vortices. In Fig. 2a the screen contracts downstream of the local flow but in Fig. 2b it expands. Through the 'de Laval' nozzles formed inside the cocoon, the flow passes successively through several weak shocks and thus it is never far away from the sonic value. The sonic surfaces are oblique. Whereas they appear very close to the vortical motions, there is little correlation between their locations and the location of the pinch in the boundary. This is because part of the kinetic energy participates in the vortical motion of the flow and the simple consideration of the nozzle flow does not hold any further. These features are observed in the numerical models (*e.g.*, Lind 1986).

3. Concluding Remarks

Although it is not obvious from our stationary model, it is quite likely that the undulations of the pinched cocoon boundary (*i.e.*, the surface of contact discontinuity)

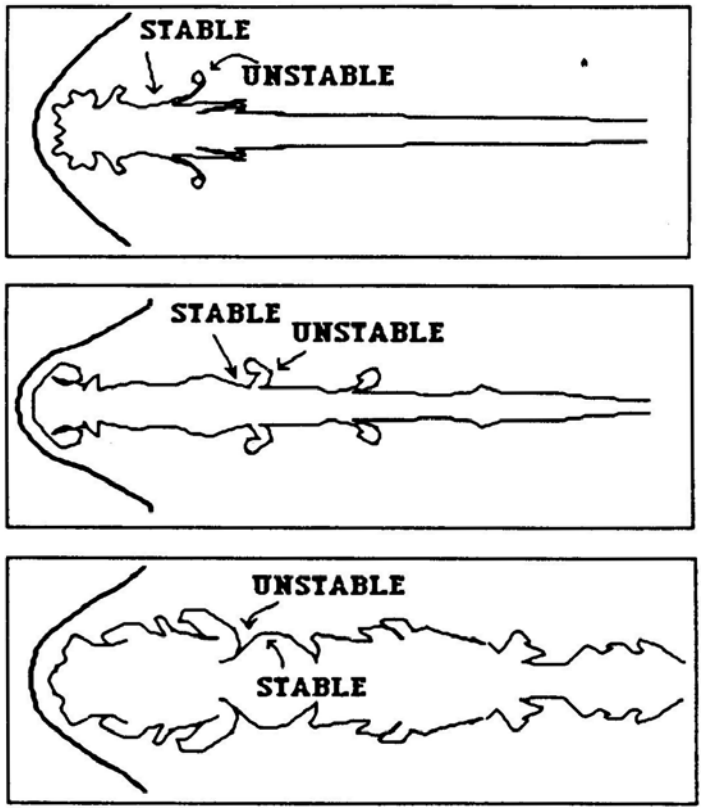

Figure 4. The contact discontinuity of M_j = 12 simulation of hydrodynamic, jets by Norman *et al.* (1985) are traced when η =10(upper panel), η = 1 (middle panel) and η= 0.1,where η is here the ratio of jet density to the external medium density. The inversion of the direction in which the spikes grow as η is varied indicates the presence of the Rayleigh-Taylor instability which may have been turned on by mechanism drawn in Fig. 3.

will grow into nonlinear regime both due to the shear of the vortex sheet and the local centrifugal acceleration of the vortical motions. Fig. 3 shows how the non-linearity due to the Rayleigh-Taylor instability may be selectively turned on depending upon whether the jet is light or heavy. The nonlinear development of the 'spikes' always takes place from the denser medium to the lighter medium. Thus, for example, for a highly supersonic jet, the spikes should point towards the jet when the jet is light and away from the jet when the jet is heavy. (For mildly supersonic jet the dissipation may wash out the effects discussed here.) In Fig. 4 we trace the contact discontinuity of some simulations of the hydrodynamic jets by Norman *et al.* (1985), to show that our conjecture is probably correct. Simulations of Lind (1986) also show similar features. In all the simulations one observes the oblique shocks and the Mach number of the flow inside the cocoon is very close to the unity, exactly as is derived in this paper. Although this implies that the instabilities will grow indefinitely, in reality the presence of dissipation and magnetic field may inhibit such growth to a finite amplitude. In the radio lobes the oblique shocks inside the cocoon could be the site of the electron accelerations powering the radio sources. The repeated reconnection of the magnetic field lines at the locations of the nonlinear growth may also supply sufficient power. The latter assertions could only be verified by the numerical simulation of hydromagnetic jets with dissipation taken into account.

Acknowledgement

The author acknowledges the NSF grants AST86-15325 and AST85-19411 and a Tolman fellowship with Caltech and the financial support from the International Atomic Energy Agency.

References

Baird, J. P. 1987 *Proc. R. Soc. London*, Ser.A, **409,** 59.
Blandford, R., Rees, M. 1974, *Mon. Not. R. astr. Soc*, **169,** 395.
Broadbent, E. G., Moore, D. W. 1987, *Proc. R. Soc. London*, Ser.A, **409,** 47.
Chakrabarti, S. K. 1988, *Mon. Not. R. astr. Soc.*, (In press).
Clarke, D. A., Norman, M. L., Burns, J. O., 1986, *Astrophys. J.* (Lett.), **311,** L63.
Dreher, J. W., Carilli, C. L., Perley, R. A. 1987, *Astrophys. J.*, **316,** 611.
Lamb, H., 1932, *Hydrodynamics*, Cambridge University Press.
Liepmann, H. W., Roshko, A., 1956, *Elements Of Gas Dynamics*, Wiley, New York.
Lind, K. 1986, *Ph.D. Dissertation*, Calif. Inst, of Technology.
Norman, M. L., Winkler, K.-H. A., 1985, *Bull. Los Alamos Lab.*, **12**, 38.
Norman, M. L., Winkler, K.-H. A, Smith, M. D., 1982, *Astr. Astrophys.*, **113,** 285.
William, A. G., Gull, S. F., 1984, *Nature*, **310,** 33.
William, A. G., Gull, S. F., 1985, *Nature*, **313,** 33.